IRSTI 29.17.15 https://doi.org/10.26577/phst202613111

Peculiarities of diffusive and convective mixing in gas mixtures with fine dust in isobaric-isothermal conditions

V. Mukamedenkyzy[1], H. Altenbach[2], A. Tolepbergen[1*] and V. Kossov[3]

[1]Al Farabi Kazakh National University, Almaty, Kazakhstan
[2]Otto von Guericke University, Magdeburg, Germany
[3]Abai Kazak National Pedagogical University, Almaty, Kazakhstan
*e-mail: arsen4236@gmail.com

(Received January 12, 2026; received in revised form May 9, 2026; accepted May 16, 2026)

This paper presents a numerical study of diffusive–convective mixing in gas–solid systems under isothermal and isobaric conditions. Two model systems, CO_2 + Si – N_2 and H_2O + C – Air, were investigated to analyze the transport of gas components and dispersed solid particles. Simulations were performed in the ANSYS Fluent environment using the Species Transport and Eulerian Multiphase Flow models, enabling the coupled description of gas-phase diffusion and particle motion. Calculations were carried out for a two-dimensional vertical channel geometry previously employed in studies of gas–gas mixing, where instability of mechanical equilibrium in the diffusion layer was observed. The results show that the dispersed solid phase forms localized regions of increased density that subsequently undergo gravitational displacement, leading to the development of convective structures and intensive mixing. At later stages, the system evolves toward a quasi-stationary concentration distribution. The study extends a previously validated numerical approach for gas mixtures to gas–solid media with different physicochemical properties and demonstrates the formation of Rayleigh–Taylor-type structures in the absence of thermal and chemical effects. The proposed methodology provides an effective tool for modeling diffusion–convective processes in multiphase systems and may be applied to the analysis of aerosol transport and dust particle dynamics in both atmospheric and technological environments.

Keywords: diffusion, convection, instability, Eulerian model, numerical modeling, ANSYS fluent, Rayleigh-Taylor instability.

1. Introduction

Diffusion and convective mass transfer in gas–solid systems play a critical role in a wide range of natural and industrial processes, including atmospheric aerosol transport, dust emission from thermal power plants, and mixing in chemical reactors. In many practically relevant scenarios, these processes occur under isothermal and isobaric conditions, yet their dynamics remain poorly understood due to the complex interplay between concentration-driven instabilities and gravitational settling of the dispersed phase.

In isothermal multicomponent gas mixtures, a substantial difference in the diffusion coefficients of the components can disrupt the mechanical equilibrium of the system [1–3]. Depending on the relationship between the partial concentration gradients and the thermophysical parameters of the mixture, regions of elevated or reduced density may form [4, 5], triggering concentration-driven gravitational convection. The threshold conditions for this instability can be determined experimentally [6], analytically within the framework of Rayleigh stability theory [1, 7], or numerically [8, 9]. A comprehensive review of this phenomenon for gas mixtures is given in [10].

Previous studies [1, 10] addressed the case in which the mixture density decreases with height – a configuration that suppresses gravitational instability. The present work focuses on the opposite situation: a density gradient directed upward, which

gives rise to Rayleigh–Taylor convection. Identifying the thermophysical parameter ranges in which convective contributions to mass transfer are negligible is of direct practical importance, as it defines the experimental conditions under which mutual diffusion coefficients can be reliably determined.

When the density gradient is directed such that the heavier phase is positioned above the lighter one, the system becomes susceptible to Rayleigh–Taylor instability [11]. In gas–solid mixtures, this instability takes a distinctive form: the dispersed solid phase generates local density inversions that drive the formation of descending particle jets, clump structures, and vortex cells. While Rayleigh–Taylor dynamics have been extensively studied in gas–liquid and gas–gas configurations [12–14], the corresponding behavior in gas–solid systems – where interphase momentum exchange, buoyancy, and particle inertia act simultaneously – has received considerably less attention.

Experimental investigation of such processes is hindered by the optical opacity of particle-laden media, micro-scale interfacial effects, and the inherently non-stationary character of the phase boundary [15–18]. Computational fluid dynamics (CFD) methods provide a viable alternative, enabling detailed resolution of multicomponent and multiphase flows. However, existing numerical models frequently rely on simplified approximations or empirical closures that limit predictive accuracy for stratified gas–solid flows [19–23].

The present work addresses this gap by proposing a physically consistent numerical model for diffusion-convective mixing in binary gas mixtures containing a dispersed solid phase. The approach combines the Species Transport formulation – previously validated for ternary gas systems [24, 25] – with the Eulerian Multiphase Flow method, which accounts for interphase momentum exchange without the need for empirical corrections. Two representative systems are examined: CO_2 + Si – N_2 at T = 300 K and H_2O + C – Air at T = 393 K, both modelled under isobaric conditions at p = 0.1 MPa with initial solid-phase volume fractions of 1%, 2.5%, and 5%. The objective is to characterize the universal stages of flow evolution, quantify the influence of particle loading on gas-phase transport, and establish the conditions under which Rayleigh–Taylor-like convective structures emerge in gas–solid media.

2. Mathematical model and numerical methods

The system under study consists of two cylindrical vessels arranged vertically and connected by a thin cylindrical channel. At the initial moment of time, the upper vessel is filled with a mixture of gases (CO_2 or H_2O) and solid microparticles (Si or C), and the lower vessel contains pure N_2 or air. After the partition between the vessels is opened, the components interpenetrate under the action of concentration gradients and gravitational forces.

The process proceeds under isothermal and isobaric conditions. The interaction between phases is described by volume fractions and momentum exchange. The solid phase is modelled as a dispersed medium with spherical particles with a diameter of d_p=10^{-5} m. The initial volume fractions of solid particles in the upper vessel are 1%, 2.5%, and 5%. The selected initial particle volume fractions (1%, 2.5% and 5%) correspond to a dilute and moderately loaded dispersed phase regime. This range was chosen to evaluate the influence of particle loading on the evolution of diffusion-convective structures while remaining within the applicability limits of the adopted Eulerian multiphase approach without introducing additional submodels for agglomeration, hindered settling, or dense granular interactions. At these concentrations, the solid phase already produces a noticeable contribution to the local density stratification and interphase momentum exchange, but the system does not yet transition to a densely packed regime. At particle concentrations exceeding approximately 10%, one may expect stronger interparticle effects, partial suppression or restructuring of convective cells, and a substantial increase in the role of collective settling and nonlinearity of momentum exchange. Detailed thermophysical properties of gases and solid particles can be found in Table 1.

Table 1. Physicochemical properties of gases and particulate matter for the systems CO_2 + Si – N_2 and H_2O + C – Air.

Component	Phase type	Molar mass, g/mol	Density, kg/m³	Viscosity, Pa·s	Thermal conductivity, W/(m·K)	c_p, J/(kg·K)
CO_2	gas	44.01	1.977	1.48×10^{-5}	0.0166	844
Si	solid	28.09	2330	–	148	700
N_2	gas	28.02	1.165	1.76×10^{-5}	0.0259	1040
H_2O (steam)	gas	18.02	0.804	2.00×10^{-5}	0.025	1995
C	solid	12.01	2000	–	6	710
Air	gas	28.97	1.161	1.85×10^{-5}	0.026	1005

Based on the thermophysical parameters presented in Table 1, a computational model of diffusion-convective mixing was developed. The spatial configuration of the system, reproducing the mutual arrangement of the flasks and the connecting channel, is shown in Figure 1.

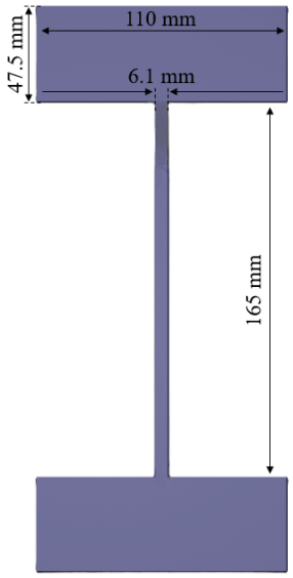

Figure 1. Geometric model of the study area.

The geometry of the area (Fig. 1) is two-dimensional and axisymmetric: the height of each vessel is 47.5 mm, the height of the connecting channel is 70 mm, and the diameter of the channel is 6.1 mm. The walls are considered impermeable and adhesive to particles, without slippage or heat exchange.

3. Basic equations of the model

The calculation method is based on a previously verified gas diffusion model [24, 25], extended in the present work to account for the solid dispersed phase. The gas-phase transport of species is described by the Species Transport equations under isothermal and isobaric conditions, with turbulence modelled using the *k–ω SST* approach. To incorporate the solid phase, the Eulerian Multiphase Flow framework is adopted, in which each phase – gas and solid – is treated as an interpenetrating continuum with its own velocity, pressure, and volume fraction fields.

Mass conservation for phase q is expressed by the continuity equation:

$$\frac{\partial}{\partial t}(\alpha_q\rho_q)+\nabla\cdot(\alpha_q\rho_q\vec{v}_q)= =\sum_{p=1}^{n}(\dot{m}_{pq}-\dot{m}_{qp})+S_q \quad (1)$$

where $\vec{v}_q$ – phase transition rate and $\dot{m}_{pq}$ characterizes mass transfer from phase p to phase q, and $\dot{m}_{qp}$ characterizes mass transfer from phase q to phase p and these mechanisms can be specified separately [26]. In the present configuration, no phase transition or chemical reaction occurs, so these terms vanish identically.

The momentum balance for phase q takes the form:

$$\frac{\partial}{\partial t}(\alpha_q\rho_q\vec{v}_q)+\nabla\cdot(\alpha_q\rho_q\vec{v}_q\vec{v}_q)= =-\alpha\nabla p+\nabla\cdot\bar{\bar{\tau}}_q+\alpha_q\rho_q\vec{g}+ +\sum_{p=1}^{n}(\vec{R}_{pq}+\dot{m}_{pq}\vec{v}_{pq}-\dot{m}_{qp}\vec{v}_{qp})+ +(\vec{F}_q+\vec{F}_{lift,q}+\vec{F}_{wl,q}+\vec{F}_{vm,q}+\vec{F}_{td,q}) \quad (2)$$

where the stress–strain tensor, effective phase density, and standard body-force contributions are defined according to the Eulerian multiphase formulation [26]. The gravitational term plays a central role in the present problem, as the density inversion between the particle-laden upper region and the pure gas in the lower flask drives the Rayleigh–Taylor-like instability observed in the results.

Interphase momentum exchange between the gas and solid phases is described by:

$$\sum_{p=1}^{n} \vec{R}_{pq} = \sum_{p=1}^{n} K_{pq}(\vec{v}_p - \vec{v}_q) \tag{3}$$

where K_{pq} is the interphase momentum exchange coefficient, determined from the Schiller–Naumann drag correlation for spherical particles of diameter d_p=10^{-5} m. This term is the primary coupling mechanism between the two phases and governs the rate of gravitational particle settling and the feedback of particle drag on the gas velocity field.

The volume fraction of each phase is obtained by solving the transport equation:

$$\frac{1}{\rho_{rq}}\left(\frac{\partial}{\partial t}(\alpha_q \rho_q) + \nabla \cdot (\alpha_q \rho_q \vec{v}_q) = \sum_{p=1}^{n} (\dot{m}_{pq} - \dot{m}_{qp})\right) \tag{4}$$

subject to the constraint that volume fractions sum to unity across all phases. This equation is solved for each secondary phase; the primary phase fraction is then determined algebraically.

The momentum balance for the solid phase s, accounting for particle pressure and granular stresses, is given by:

$$\begin{aligned} &\frac{\partial}{\partial t}(\alpha_s \rho_s \vec{v}_s) + \nabla \cdot (\alpha_s \rho_s \vec{v}_s \vec{v}_s) = \\ &= -\alpha_s \nabla p - \nabla p_s + \nabla \cdot \bar{\bar{\tau}}_s + \alpha_s \rho_s \vec{g} + \\ &+ \sum_{l=1}^{N} (K_{ls}(\vec{v}_l - \vec{v}_s) + \dot{m}_{ls}\vec{v}_{ls} - \dot{m}_{sl}\vec{v}_{sl}) + \\ &+ (\vec{F}_s + \vec{F}_{lift,s} + \vec{F}_{wl,s} + \vec{F}_{vm,s} + \vec{F}_{td,s}) \end{aligned} \tag{5}$$

where p_s – solid particle pressure s, $K_{ls} = K_{sl}$ – momentum exchange coefficient between liquid or solid phase l and solid phase s, N – total number of phases.

The rheological behaviour of the solid phase is described within the kinetic theory of granular flows. By analogy with molecular motion in a gas, the random translational velocity of particles arising from inter-particle collisions is characterised by a granular temperature Θ_s, defined as one third of the mean square of the particle velocity fluctuation. This quantity governs the effective pressure, viscosity, and normal stresses of the solid phase, and accounts for the partially inelastic nature of inter-particle collisions. The granular temperature is solved as an additional transport equation coupled to the momentum balance (5).

4. Boundary and initial conditions

At the initial moment:

- upper region: mixture of gas (CO_2 or H_2O) and dust from solid particles (Si or C);
- lower region and channel: pure gas (N_2 or Air);

On the walls:

$$u_q = 0, \ \frac{\partial Y_i}{\partial n} = 0 \tag{6}$$

For particles – no-slip boundary condition. Pressure and temperature are assumed to be constant: p=0.1 MPa, T=300 K (CO_2+Si–N_2) and T=393 K (H_2O+C–Air).

5. Numerical implementation

The calculation was performed in a non-stationary setting, which made it possible to track the dynamics of mixing and phase transfer over time. The time step was 1 s, and the total number of integration steps in time was 1200, which corresponds to 20 minutes of real time of the process. This time interval was chosen to make it possible to track the transition of the system from the initial unstable state to a quasi-steady-state distribution of concentrations.

The calculations used a pressure-based coupled solver with full coupling between the pressure and velocity fields. The Second Order Upwind scheme

was used to approximate convective terms, and the PRESTO! scheme was used for pressure, providing increased accuracy in the presence of gravitational effects. Time discretization was implemented using the Second Order Implicit scheme, which ensured the stability of the solution at the selected time step.

The computational grid had a structured topology and contained 164 120 cells and 165 974 nodes. The minimum cell size in the channel area was 0.25 mm, which ensured correct resolution of local concentration and velocity gradients at interphase boundaries. Convergence criteria for all equations were set at no higher than 10^{-6} for velocity and pressure fields, and 10^{-8} for concentrations and volume fractions of phases.

6. Results and discussion

The mixing process in both systems considered – CO_2 + Si – N_2 and H_2O + C – Air – is characterized by pronounced non-stationarity and multi-stage evolution. Almost immediately after the start of the calculation, a contact zone with contrasting densities forms, causing a disturbance in mechanical equilibrium and the formation of downward and upward flows. In the first seconds of the calculation, gas from the upper flask begins to penetrate the lower flask, while the solid phase settles under the action of gravity.

The spatial evolution of both phases is illustrated in Figs. 2 and 3 for the CO_2 + Si – N_2 and H_2O + C – Air systems, respectively, at four time instants: t = 30, 60, 90, and 120 s.

For the gas phase (Figs. 2a and 3a), the concentration front descends progressively through the connecting channel. At t = 30 s, the CO_2 (or H_2O) distribution is already non-uniform along the channel axis, with a distinct concentration gradient visible between the upper and lower regions. By t = 60–90 s, the front reaches the lower flask and begins to spread laterally, driven by the combined action of diffusion and the developing convective flow. The H_2O + C – Air system (Fig. 3a) shows a visibly more advanced penetration front at equivalent time steps, consistent with the higher gas-phase transfer rates reported in Table 2 and attributable to the lower molar mass and higher diffusion mobility of water vapor.

The solid phase dynamics (Figs. 2b and 3b) present a qualitatively different picture. At t = 30 s, the particles have already concentrated into a narrow elongated region within the channel, indicating rapid gravitational settling from the upper flask. At t = 60 s, a compact high-concentration cluster is clearly visible at the channel exit – this structure corresponds to the moment of maximum local solid-phase density prior to its entry into the lower flask. By t = 90 s, the cluster detaches and enters the lower flask, adopting the characteristic teardrop morphology discussed in relation to Fig. 5. For the C particles in the H_2O system (Fig. 3b), this sequence occurs approximately 7–10 s earlier compared to Si in the CO_2 system, reflecting the influence of gas viscosity and density on particle settling dynamics. At t = 120 s, the solid phase in both systems has largely accumulated at the bottom of the lower flask, with only a residual thread remaining in the channel.

In general, the behavior of the systems is consistent with diffusion-convection processes in a gravitational field, where concentration and density gradients act simultaneously. Already in the early stages of the calculation, Rayleigh–Taylor instabilities form, manifesting themselves in the form of local wave-like deformations of the gas interface, which then transition into elongated convective jets.

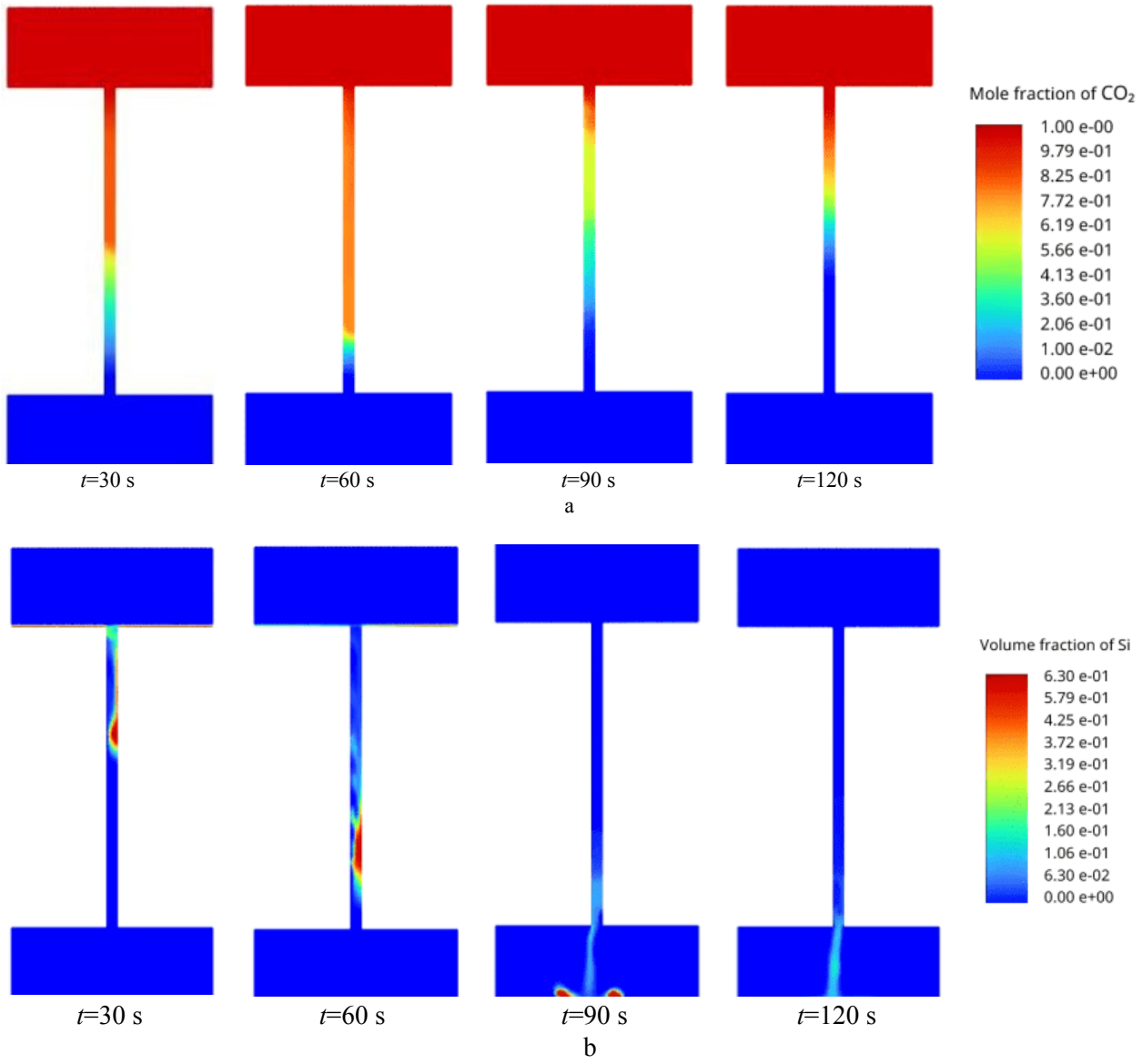

Figure 2. Gas/solid particle movement for the system CO_2 + 0.025 Si – N_2 at p=0.1 MPa, T=300 K depending on the time:
a) concentration change of CO_2; b) concentration change of Si.

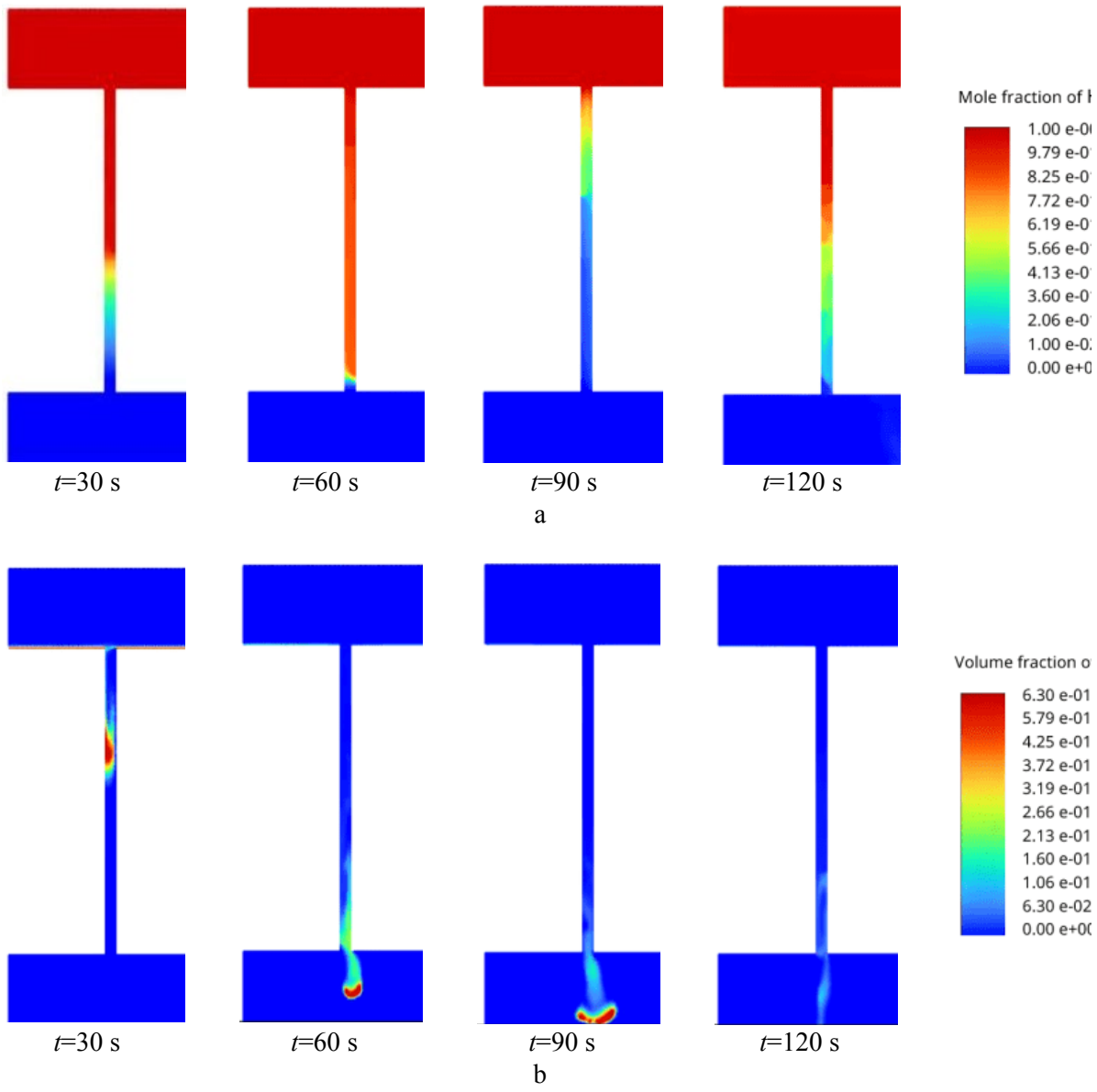

Figure 3. Gas/solid particle movement for the system H_2O + 0.025 C – Air at p=0.1 MPa, T=393 K depending on the time:
a) concentration change of H_2O; b) concentration change of C.

Upon opening of the partition, CO_2 (or H_2O) undergoes immediate penetration into the lower flask, driven by the concentration gradient across the channel. Within the first seconds, the volume-averaged mole fraction of CO_2 in the lower flask reaches approximately 0.035 – a value established quasi-instantaneously relative to the total process duration. This rapid onset reflects the dominant role of molecular diffusion prior to the development of convective structures. The solid phase remains largely confined to the upper flask during this interval, exhibiting negligible transfer to the lower volume.

The redistribution of the dispersed phase within the upper flask generates local regions of elevated density near the bottom wall. The resulting density inversion triggers Rayleigh–Taylor-type instability, manifesting as elongated convective jets visible in Figs. 2–3. For the gas phase (Fig. 4a, 4c), this stage appears as a sustained and monotonic concentration increase. The solid phase (Fig. 4b, 4d), by contrast, exhibits strongly oscillatory behavior with

characteristic fluctuations in the range 200–500 s, peak amplitude reaching ~0.025–0.026 for Si and ~0.023–0.025 for C. This contrast in kinetic behavior – smooth for the gas, impulsive for the particles – reflects a fundamental difference in the transfer mechanisms: gas transport is governed by diffusion-enhanced convection, whereas particle transfer occurs intermittently through gravitational avalanches associated with the evolving instability structures.

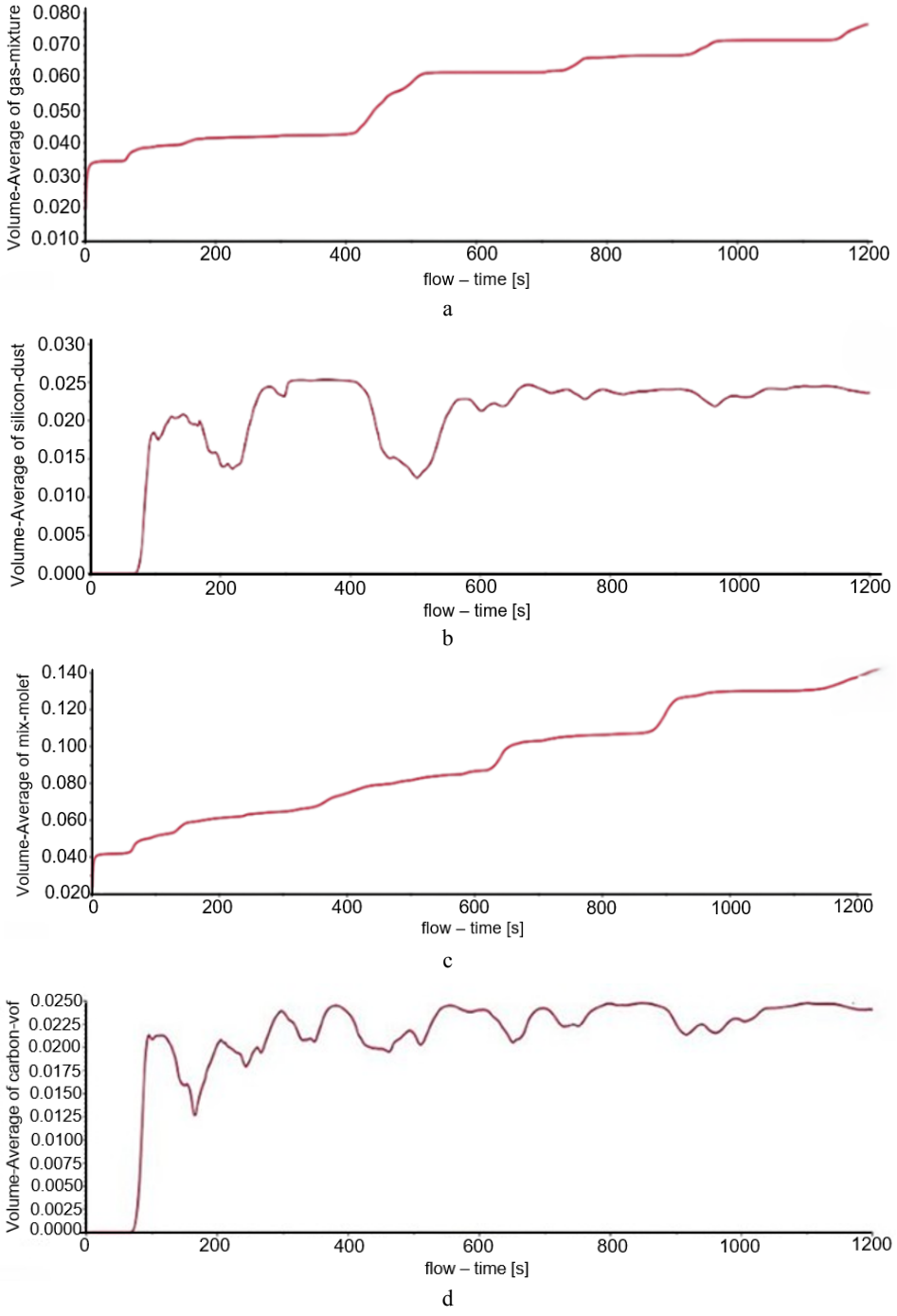

Figure 4. Dynamics of changes in the amount of gas/solid particles for systems CO_2 + 0.025 Si – N_2 at p=0.1 MPa, T=300 K and H_2O + 0.025 C – Air at p=0.1 MPa, T=393 K depending on the time in the lower flask: a) plot for CO_2; b) plot for Si; c) plot for H_2O; d) plot for C.

Both phases approach stable concentration distributions. The gas fraction in the lower flask continues to grow slowly, while solid phase oscillations decay and converge to a near-constant value. At t = 1200 s, the volume fraction of particles in the lower flask reaches 95–99% of the total injected particle mass, confirming near-complete gravitational settling.

Table 2 reveals a clear and quantitatively significant inverse relationship between initial solid-phase volume fraction and the extent of gas-phase transfer. For the CO_2 + Si – N_2 system, the mole fraction of CO_2 in the lower flask at t = 1200 s decreases from 0.1179 at φ = 1% to 0.0764 at φ = 2.5% and 0.0439 at φ = 5% – a reduction by a factor of 2.7 across the studied range. This trend indicates that higher particle loading progressively suppresses convective gas transport, likely through increased momentum dissipation in the dispersed-phase continuum and partial disruption of coherent convective structures. A symmetric but less pronounced effect is observed for the H_2O + C – Air system (Table 2).

Table 2. The amount of gas/solid particle diffusing from one chamber to another.

System	CO_2	Si	N_2	System	H_2O	C	Air
CO_2 + 0.050 Si – N_2	0.0439	0.04980	0.8990	H_2O + 0.050 C – Air	0.0425	0.0396	0.8102
CO_2 + 0.025 Si – N_2	0.0764	0.02364	0.8812	H_2O + 0.025 C – Air	0.1377	0.0240	0.7944
CO_2 + 0.010 Si – N_2	0.1179	0.00998	0.7813	H_2O + 0.010 C – Air	0.2496	0.0101	0.6997

Under identical geometric and boundary conditions, the H_2O + C – Air system consistently exhibits higher gas-phase transfer relative to CO_2 + Si – N_2. At φ = 1%, the mole fraction of H_2O in the lower flask (0.2496) is approximately 2.1 times higher than that of CO_2 (0.1179). This difference is attributable to the lower molar mass and higher diffusion mobility of water vapor compared to CO_2, which leads to a larger diffusion-driven contribution at early stages and faster convective onset. The qualitative flow structure, however, remains identical between the two systems, confirming the universality of the observed instability mechanism.

A particularly notable finding concerns the timing of teardrop-shaped particle cluster formation in the lower flask (Fig. 5). For both systems and both φ = 1% and φ = 2.5%, the cluster appears at t ≈ 82.5 s, while at φ = 5% it forms marginally earlier at t ≈ 75.0 s – a difference of only 9%. This near-independence of cluster formation time from initial solid-phase concentration suggests that the onset of Rayleigh–Taylor-like instability is governed primarily by hydrodynamic factors – the density inversion threshold and gravitational acceleration – rather than by the quantity of dispersed material. The consistent timing across both chemical systems further supports the interpretation of this phenomenon as a universal structural feature of gas–solid convective instability under the given geometric and thermodynamic constraints.

The results obtained are consistent with general ideas about the behavior of dispersed phases in gravitational flows and demonstrate the possibility of using the *ANSYS Fluent* numerical model based on a combination of Species Transport and Eulerian Multiphase Flow to describe such processes without the use of experimental data.

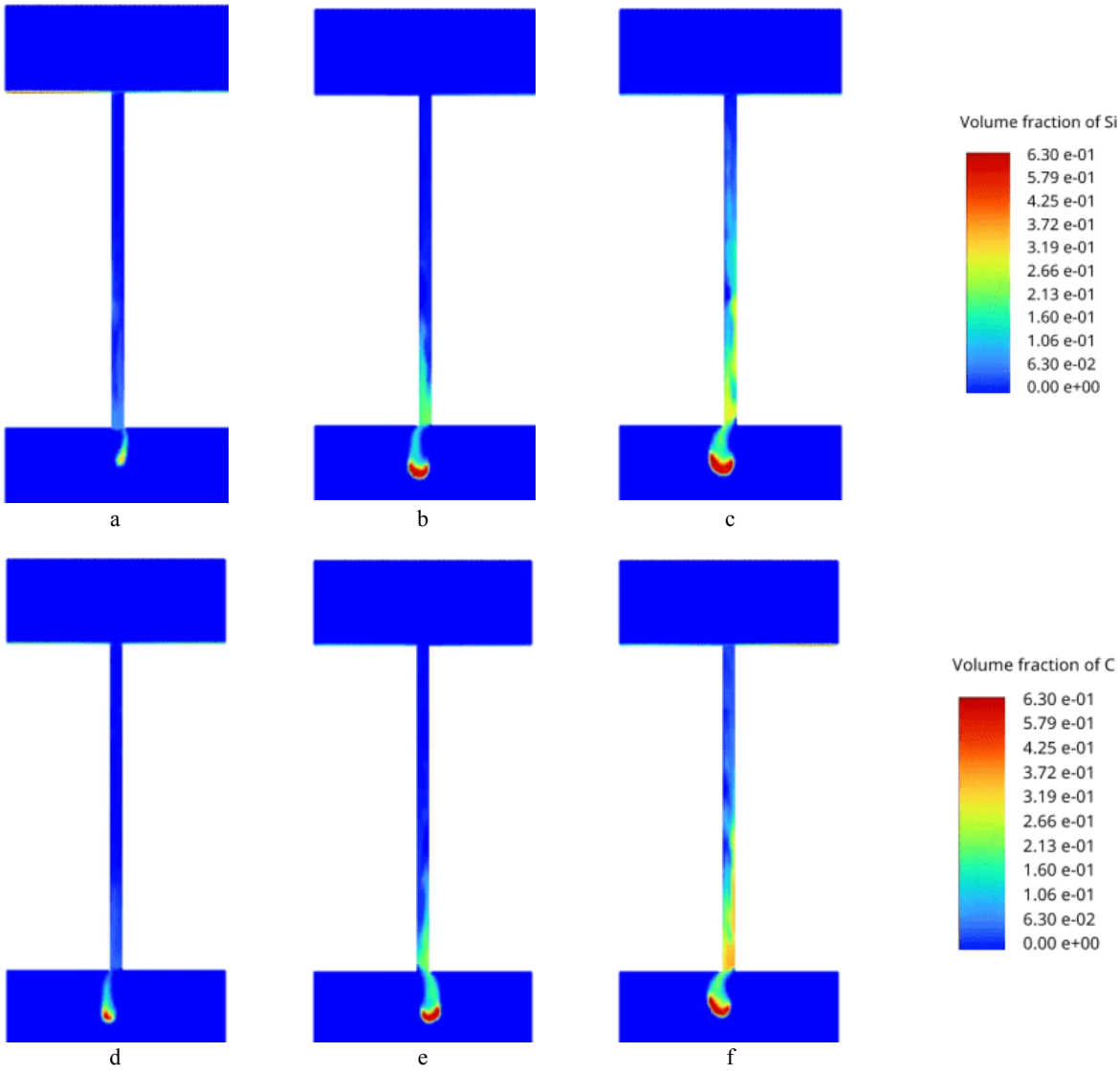

Figure 5. The moment of formation of a teardrop-shaped solid phase structure in the lower flask: a) CO_2 + 0.010 Si – N_2 (t=82.5 s); b) CO_2 + 0.025 Si – N_2 (t=82.5 s); c) CO_2 + 0.050 Si – N_2 (t=75.0 s); d) H_2O + 0.010 C – Air (t=82.5 s); e) H_2O + 0.025 C – Air (t=82.5 s); f) H_2O + 0.050 C – Air (t=75.0 s).

7. Conclusion

This paper presents a numerical study of diffusion-convective mixing in multiphase systems containing gas and solid dispersed components. Modeling was performed under isothermal and isobaric conditions using a combined approach based on the integration of Species Transport and Eulerian Multiphase Flow models in the *ANSYS Fluent 2025 R1* environment.

Two systems are considered: CO_2 + Si – N_2 and H_2O + C – Air, which differ in terms of the temperature and physical properties of the gas phase. The same qualitative patterns of flow evolution have been established for both systems. At the initial stage, gas diffusion into the lower flask and sedimentation of solid particles under the action of gravity are observed. At subsequent stages, convective structures typical of Rayleigh–Taylor instability are formed, which is confirmed by the formation of droplet-like solid phase formations in the channel. It is shown that the moment of formation of structural aerosol formations practically coincides for both systems and does not

depend on the initial concentration of solid particles (1%, 2.5%, 5%), which indicates the dominant role of hydrodynamic factors and density inversion of the mixture in the development of the flow structure.

A comparison with a previously verified model showed a qualitative match in the dynamics and time scales of mixing, confirming the correctness of the numerical approach used [21].

The results obtained are of fundamental importance, as they allow determining the ranges of thermophysical parameters in which reliable determination of mutual diffusion coefficients is possible. These coefficients are key transport constants that affect the accuracy of calculations when modeling various multiphase and multicomponent systems. Thus, this study contributes to the refinement of diffusion transport parameters and expands our understanding of the laws of mass transfer in gas-solid media.

The developed methodology can be used to analyze gas-solid diffusion processes of various nature–from laboratory experiments to problems related to aerosol mixture emissions from thermal power plants. A promising direction for further research is the inclusion of heat exchange, reaction effects, and the transition to three-dimensional geometry for a more complete description of the dynamics of mixing and sedimentation of solid particles.

Acknowledgements

The work was supported by the Committee of Science of the Ministry of Science and Higher Education of the Republic of Kazakhstan, project AP23488139.

Conflicts of interest

The authors declare no conflict of interest.

Author contributions

Conceptualization, V.N.K.; Methodology, A.T.; Software, A.T.; Validation, A.T.; Formal Analysis, A.T., V.N.K., V.M. and H.A.; Investigation, A.T.; Resources, V.N.K., V.M.; Data Curation, A.T.; Writing – Original Draft Preparation, A.T. and H.A.; Writing – Review & Editing, V.N.K. and V.M.; Visualization, A.T.; Supervision, V.N.K., V.M. and H.A.; Project Administration, V.N.K.; Funding Acquisition, V.N.K.

References

1. V. N. Kosov and V. D. Seleznev, *Anomalous Occurrence of Free Gravitational Convection in Isothermal Ternary Gas Mixtures*. Ekaterinburg, Russia: Ural Branch of the Russian Academy of Sciences, 2004.

2. V. V. Dil'man, D. A. Lipatov, V. A. Lotkhov, et al., "Instability in unsteady-state evaporation of binary solutions into an inert gas," *Theor. Found. Chem. Eng*., vol. 39, no. 6, pp. 566–572, 2005, https://doi.org/10.1007/s11236-005-0118-0

3. S. Bolegenova, A. Askarova, N. Slavinskaya, S. Ospanova, A. Maxutkhanova, A. Aldiyarova, and D. Yerbosynov, "Statistical modeling of spray formation, combustion, and evaporation of liquid fuel droplets," *Phys. Sci. Technol*., vol. 9, no. 3–4, pp. 69–82, 2022, https://doi.org/10.26577/phst.2022.v9.i2.09

4. V. A. Kaminskii, "Special modes of three-component diffusion in gases," *Russ. J. Phys. Chem. A,* vol. 85, no. 12, pp. 2203–2208, 2011, https://doi.org/10.1134/S0036024411120156

5. V. N. Kosov, Yu. I. Zhavrin, and V. D. Seleznev, "Inversion of the density gradient and the 'gate' in isothermal mixing of gases," *Tech. Phys., vol*. 43, no. 5, pp. 488–492, 1998.

6. V. N. Kosov, Yu. I. Zhavrin, D. U. Kul'zhanov, and K. K. Karataeva, "Effect of pressure on the type of mixing in a three-component gas mixture containing a real gas component," *Tech. Phys. Lett.*, vol. 26, no. 12, pp. 1108–1109, 2000.

7. V. N. Kosov, O. V. Fedorenko, Yu. I. Zhavrin, and V. Mukamedenkyzy, "Instability of mechanical equilibrium during diffusion in a three-component gas mixture in a vertical cylinder," *Tech. Phys.*, vol. 59, no. 4, pp. 482–486, 2014, https://doi.org/10.1134/S1063784214040161

8. A. Zhussanbayeva, V. N. Kossov, O. V. Fedorenko, and M. Zhaneli, "Instability of mechanical equilibrium and concentration convection in isothermal ternary gaseous systems," *Phys. Sci. Technol.*, vol. 9, no. 1–2, pp. 55–61, 2022, https://doi.org/10.26577/phst.2022.v9.i1.07

9. M. Moldabekova, V. Mukamedenkyzy, M. Asembayeva and A. Tolepbergen, "Investigation of the diffusion of two gases equally diluted with different ballast gases," *Recent Contrib. Phys*., vol. 89, no. 2, pp. 57–61, 2024, https://doi.org/10.26577/RCPh.2024v89i2-08

10. V. N. Kossov and H. Altenbach, "Diffusion mechanisms of convective instability in liquid and gas mixtures," *J. Appl. Math. Mech*., vol. 103, no. 11, Art. no. e202300801, 2023, https://doi.org/10.1002/zamm.20230080

11. A. Banerjee, "Rayleigh–Taylor instability: A status review of experimental designs and diagnostics," *J. Fluids Eng*., vol. 142, no. 12, Art. no. 120801, 2020, https://doi.org/10.1115/1.4048349

12. S. A. Bazarbekov, "Application of high-speed gas-flame technology for surface hardening," *Phys. Sci. Technol*., vol. 8, no. 1–2, pp. 47–52, 2021, https://doi.org/10.26577/phst.2021.v8.i1.06

13. S. Balachandar and J. K. Eaton, “Turbulent dispersed multiphase flow,” *Annu. Rev. Fluid Mech*., vol. 42, pp. 111–133, 2010, https://doi.org/10.1146/annurev.fluid.010908.165243

14. J. Capecelatro et al., “Gas–particle dynamics in high-speed flows: A review,” *Annu. Rev. Fluid Mech*., vol. 56, pp. 379–403, 2024, https://doi.org/10.1146/annurev-fluid-121021-015818

15. L. Villafañe, A. Aliseda, S. Ceccio, P. Di Marco, N. Machicoane, and T. J. Heindel, “Experimental methods for dispersed multiphase flows,” *Int. J. Multiphase Flow*, vol. 189, Art. no. 105239, 2025, https://doi.org/10.1016/j.ijmultiphaseflow.2025.105239

16. Y. Yan, K. Mohanarangam, W. Yang, and J. Tu, “Experimental measuring techniques for industrial-scale multiphase flow problems,” *Exp. Comput. Multiph. Flow*, vol. 6, pp. 1–13, 2024, https://doi.org/10.1007/s42757-023-0172-z

17. S. Bolegenova, A. Askarova, S. Ospanova, et al., “Technology of reducing greenhouse gas emissions,” *Phys. Sci. Technol*., vol. 11, no. 1–2, pp. 64–75, 2024, https://doi.org/10.26577/phst2024v11i1a8

18. S. Tas-Koehler et al., “A critical analysis of drag force modelling for disperse gas–solid flows,” *Chem. Eng. Sci*., Art. no. 117007, 2021, https://doi.org/10.1016/j.ces.2021.117007

19. B. Akula and D. Ranjan, “Dynamics of buoyancy-driven flows at moderately high Atwood numbers,” *J. Fluid Mech*., vol. 795, pp. 313–355, 2016, https://doi.org/10.1017/jfm.2016.199

20. Y. Liang, A. Alkindi, K. Alzeyoudi, L. Liu, M. Ali, and N. Masmoudi, “Experimental investigation of three-dimensional Rayleigh–Taylor instability,” *J. Fluid Mech*., vol. 994, Art. no. A7, 2024, https://doi.org/10.1017/jfm.2024.754

21. C. Liu, Y. Zhang, and Z. Xiao, “Unified model for Rayleigh–Taylor and Richtmyer–Meshkov fingers,” *J. Fluid Mech*., vol. 954, Art. no. A13, 2023, https://doi.org/10.1017/jfm.2022.1000

22. M. L. R. Peixoto, M. S. C. A. Brito, R. J. Santos, and V. J. P. Vilar, “Kinetic model implementation in raceway pond reactors,” *Chem. Eng. Res. Des*., vol. 210, pp. 150–162, 2024, https://doi.org/10.1016/j.cherd.2024.08.030

23. P. M. Pancorbo, J. M. Ortiz de Zárate, H. Bataller, and F. Croccolo, “Gravity effects on Soret-induced fluctuations,” *Eur. Phys. J. E*, vol. 40, no. 2, Art. no. 22, 2017, https://doi.org/10.1140/epje/i2017-11513-9

24. V. N. Kossov, V. Mukamedenkyzy, A. Tolepbergen, and H. Altenbach, “Peculiarities of combined mixing caused by instability of mechanical equilibrium,” *Int. J. Chem. Eng*., Art. no. 9643371, 2025, https://doi.org/10.1155/ijce/9643371

25. V. Mukamedenkyzy and A. Tolepbergen, “Some features of Rayleigh–Taylor convection in the mixing of ideal gas mixtures,” *Recent Contrib. Phys*., vol. 92, no. 1, pp. 110–119, 2025, https://doi.org/10.26577/RCPh202592112

26. ANSYS, Inc. "*ANSYS Fluent Theory Guide 2025 R1*." ANSYS Documentation. Accessed: November 2025. [Online]. Available: https://ansyshelp.ansys.com

Information about the authors:

Venera Mukamedenkyzy – Candidate of Physical and Mathematical Sciences, Associate Professor, Al Farabi Kazakh National University (Almaty, Kazakhstan, e-mail: mukameden@inbox.ru).

Holm Altenbach – Dr.-Ing. habil., Professor, Otto von Guericke University Magdeburg (Magdeburg, Germany, e-mail: holm.altenbach@ovgu.de).

Arsen Tolepbergen (corresponding author) – 3rd year PhD student, Al-Farabi Kazakh National University (Almaty, Kazakhstan, e-mail: arsen4236@gmail.com).

Vladimir Kossov – Doctor of Physical and Mathematical Sciences, Professor, Abai Kazakh National Pedagogical University (Almaty, Kazakhstan, e-mail: kosov_vlad_nik@list.ru).